



OPEN Oxyresveratrol enhances hair regeneration in human dermal papilla cell and androgenetic alopecia mouse model

Hung Gia Tran¹, Aussavashai Shuayprom², Alisa Ruchusatsawat³, Kornvalee Meesilpavikkai⁴, Virgil A. S. H. Dalm⁵, Kriangsak Ruchusatsawat⁶ & Jongkonnee Wongpiyabovorn^{1✉}

Alopecia, or hair loss, is a common dermatological condition caused by multiple factors. Oxyresveratrol (ORV), a compound derived from the heartwood of *Artocarpus lakoocha*, is recognized for its potent antioxidant properties, with recent studies highlighting its anti-inflammatory effect across various cell types. This study aims to explore the therapeutic potential of ORV in treating alopecia. We evaluated the effects of ORV on Human Follicle Dermal Papilla Cells (HFDPCs) and an androgenetic alopecia (AGA) mouse model. Oxidative stress in HFDPCs was induced using hydrogen peroxide (H_2O_2), and dihydrotestosterone (DHT) was used to simulate AGA in both HFDPCs and C57BL/6NJcl mice. Our finding demonstrated that ORV significantly enhanced HFDPCs proliferation. In H_2O_2 -induced oxidative stress conditions, pretreatment with ORV decreased reactive oxygen species (ROS) levels and reduced the production of pro-inflammatory cytokine. In the AGA model, ORV inhibited β -Catenin phosphorylation in HFDPCs, thereby promoting hair growth and maintaining skin thickness, hair bulb size, and count in mice. Overall, ORV demonstrated anti-inflammatory and hair-regenerative effects in both *in vitro* and *in vivo* models of alopecia. These findings suggest that ORV is a promising candidate for the treatment of hair loss.

Keywords Alopecia, Anti-inflammation, Hair regeneration, Dihydrotestosterone, Oxyresveratrol

Hair loss, clinically termed alopecia, refers to the partial or complete absence of hair in areas where it normally grows. As a significant aesthetic concern in dermatology, alopecia profoundly impacts patients' quality of life, often diminishing self-confidence and affecting social interactions. Among the various forms of alopecia, alopecia areata (AA) and androgenetic alopecia (AGA) are the most types¹. AA is a non-cicatricial alopecia characterized by circular patches of hair loss². A systematic review reports a global lifetime incidence of AA at around 2%, with its prevalence increasing steadily with age³, and some studies suggest a slight predilection towards women⁴. In contrast, AGA has a genetic predisposition and results from heightened androgen sensitivity. It predominantly affects Caucasian, followed by Asians, African Americans, Native Americans, and Eskimos. In Caucasian men, the incidence of AGA rises with age, affecting 50% by the age of 50 and up to 80% by the age of 70. AGA also occurs frequently in women, with increased prevalence post-menopause^{5,6}.

The pathogenesis of AA involves a multifactorial interplay between genetic predisposition, environmental influences, and the collapse of the immune privilege of hair follicles^{7,8}. Among environmental factors, stress has been strongly implicated, leading to oxidative stress and the production of reactive oxygen species (ROS) and reactive nitrogen species (RNS)^{8,9}. ROS, such as hydroxyl radical (OH^\cdot), hydrogen peroxide (H_2O_2), and superoxide anion ($O_2^{\cdot-}$), play a significant role in initiating inflammation that can result in AA¹⁰. Oxygen-derived radicals drive acute inflammation with ROS being a key contributor to breakdown of immune privilege in hair follicles. Therefore, protecting hair follicles from the harmful environmental oxidizing agents is crucial.

¹Center of Excellence in Immune-Mediated Diseases, Division of Immunology, Department of Microbiology, Faculty of Medicine, Chulalongkorn University, Bangkok 10330, Thailand. ²Regional Medical Sciences Center 3 Nakhonsawan, Department of Medical Sciences, Ministry of Public Health, Nonthaburi, Thailand. ³Engineering Science Classroom, King Mongkut's University of Technology, Thonburi, Bangkok, Thailand. ⁴Department of Microbiology, Faculty of Medicine, Chulalongkorn University, Bangkok 10330, Thailand. ⁵Department of Immunology, Laboratory Medical Immunology, Erasmus University Medical Center, Rotterdam, The Netherlands. ⁶Medical Sciences Technical Office, Department of Medical Sciences, Ministry of Public Health, Nonthaburi, Thailand. ✉email: jongkonnee.w@chula.ac.th

AGA, the most prevalent form of hair loss, has garnered significant researcher interest. Its pathogenesis involves a complex interaction of genetic, hormonal, and molecular factors. Central to AGA is dihydrotestosterone (DHT), a potent androgen that binds to androgen receptors in hair follicles, leading to follicular miniaturization and a shortened hair growth cycle¹¹. Pro-inflammatory cytokines and proteins such as transforming growth factor-beta (TGF- β), Dickkopf related protein 1 (DKK-1), and interleukin 6 (IL-6) contribute to inflammation and follicular regression^{12,13}. Conversely, vascular endothelial growth factor (VEGF) promote hair growth by supporting angiogenesis, which ensures an adequate supply of nutrients and oxygen to hair follicles¹⁴. Additionally, the β -catenin signaling pathway plays a critical role in hair follicle development and cycling, with its dysregulation associated with impaired follicle regeneration and maintenance, contributing to hair loss in AGA¹⁵.

Oxyresveratrol (ORV), also known as 2,4,3',5'-tetrahydroxystilbene, is a phytoalexin present in large amounts in the heartwood of *Artocarpus lakoocha*. It has recently gained attention for its potent antioxidant, anti-inflammation, antibacterial, antiviral, and anticancer activities^{16,17}. Studies indicate that ORV exhibited strong antioxidative activity than resveratrol, mulberroside A, both recognized for their antioxidative properties¹⁸. Moreover, ORV has shown superior DNA protection compared to Trolox, Vitamin E-like antioxidant¹⁶. The anti-inflammatory action of ORV has been demonstrated in various human cell types, including macrophages, microglial cells, lens epithelial cells, and keratinocytes^{18–21}. ORV effectively inhibits the expression and production of pro-inflammatory cytokines, including IL-1, IL-6, and IL-8^{19,20,22,23}.

With increasing research interest in natural compounds for hair loss treatment, several active substances have been shown promise in supplementing or enhancing existing therapies. Building on previous evidence, this study aims to investigate the therapeutic potential of ORV in alopecia treatment, which has not yet been explored.

Results

Effect of oxyresveratrol on HFDPC proliferation

The proliferative effect of ORV on cells was evaluated using an MTT assay with 5,000 cells/well. ORV at a concentration of 10 μ g/ml significantly stimulated cell proliferation, yielding a proliferation rate of $116.97 \pm 8.58\%$ compared to the control ($P < 0.05$; Fig. 1a). To elucidate the biological impact of ORV on HFDPC, the mRNA expression levels of DKK1 and β -catenin were analyzed using RT-PCR. Treatment with ORV at concentrations of 5 μ g/ml and 10 μ g/ml resulted in a significant reduction in DKK1 mRNA expression, with values of 0.59 ± 0.06 ($P < 0.001$) and 0.46 ± 0.07 ($P < 0.0001$), respectively (Fig. 1b). Concurrently, ORV treatment at concentration from 1 to 10 μ g/ml led to an upregulation of β -catenin mRNA expression, though no significant differences were observed between the various dosages (Fig. 1c). The proliferative effect of ORV was further corroborated by CFSE staining. After 4 days of treatment, cells treated with ORV at 5 and 10 μ g/ml exhibited significantly lower fluorescent intensity compared to the negative control (Fig. 1d,e).

Protective effect of oxyresveratrol under oxidative stress

HFDPCs were stimulated with 200 μ M H_2O_2 to induce oxidative stress. Pretreatment with ORV significantly inhibited the mRNA expression of IL-1 β , IL-6, and IL-8, as well as the protein production of IL-6 and IL-8 (Fig. 2a–e; $P < 0.001$). To evaluate oxidative stress, ROS activity was measured by staining the cells with 2',7'-dichlorofluorescein diacetate (DCFDA). After 24 h of treatment, H_2O_2 -treated cells exhibited significantly higher mean fluorescence intensity compared to the negative control (2.48 ± 0.49 vs. 1.29 ± 0.21 ; $P < 0.01$). Pretreatment with ORV effectively prevented ROS production, resulting in no significant difference in mean fluorescence intensity between the ORV group and the negative control (Fig. 2f,g). Therefore, ORV has demonstrated anti-oxidative effect by suppressing pro-inflammatory cytokines.

Effect of oxyresveratrol in androgenetic alopecia model

To evaluate the effect of ORV on an AGA model, HFDPCs were pretreated with ORV before exposure to 100 nM DHT. Minoxidil at 10 μ g/ml served as the standard treatment control for AGA. ORV enhanced VEGF mRNA expression in a dose-dependent manner while maintaining VEGF protein levels comparable to the untreated control (Fig. 3a,b). Additionally, the expression of DKK1, a key inhibitor of hair growth, remained stable reduction at the mRNA level but exhibited a dose-dependent reduction in protein levels following ORV treatment (Fig. 3c,d). At a concentration of 10 μ g/ml, ORV significantly increased β -catenin mRNA levels and decreased AR mRNA expression under DHT exposure (Fig. 3e,f). Overall, ORV demonstrated the most beneficial effects on HFDPCs in comparison to the standard treatment.

Western blot analysis was used to further investigation into the intracellular mechanisms (Fig. 3g). ORV at 10 μ g/ml significantly reduced intracellular AR expression compared to DHT-only treated cells (6.06 ± 0.98 vs. 18.05 ± 1.84 , $P < 0.0001$) (Fig. 3h). Glycogen synthase kinase 3 beta (GSK-3 β), a negative regulator of β -catenin, prevents β -catenin degradation when phosphorylated, thereby promotes cell proliferation. ORV treatment increased the ratio of phosphorylated GSK-3 β to total GSK-3 β compared to the DHT-only group (1.09 ± 0.07 vs. 0.74 ± 0.08 , $P < 0.001$) (Fig. 3i). Additionally, the ratio of active β -catenin to total β -catenin was significantly higher in the ORV-treated group compared to the DHT-only group (0.87 ± 0.15 vs. 0.37 ± 0.09 , $P < 0.001$), showing no significant difference between the ORV-treated group and the negative control (Fig. 3j). These finding demonstrated that ORV modulated several key molecules involve in AGA.

Skin irritation test

To assess the irritant potential of ORV prior to in vivo experimentation, 3-D human epidermal tissues were utilized. Results from the MTT assay indicated that exposure to ORV solutions ranging from 1 to 100 μ g/ml did not significantly impact tissue viability (Fig. 4).

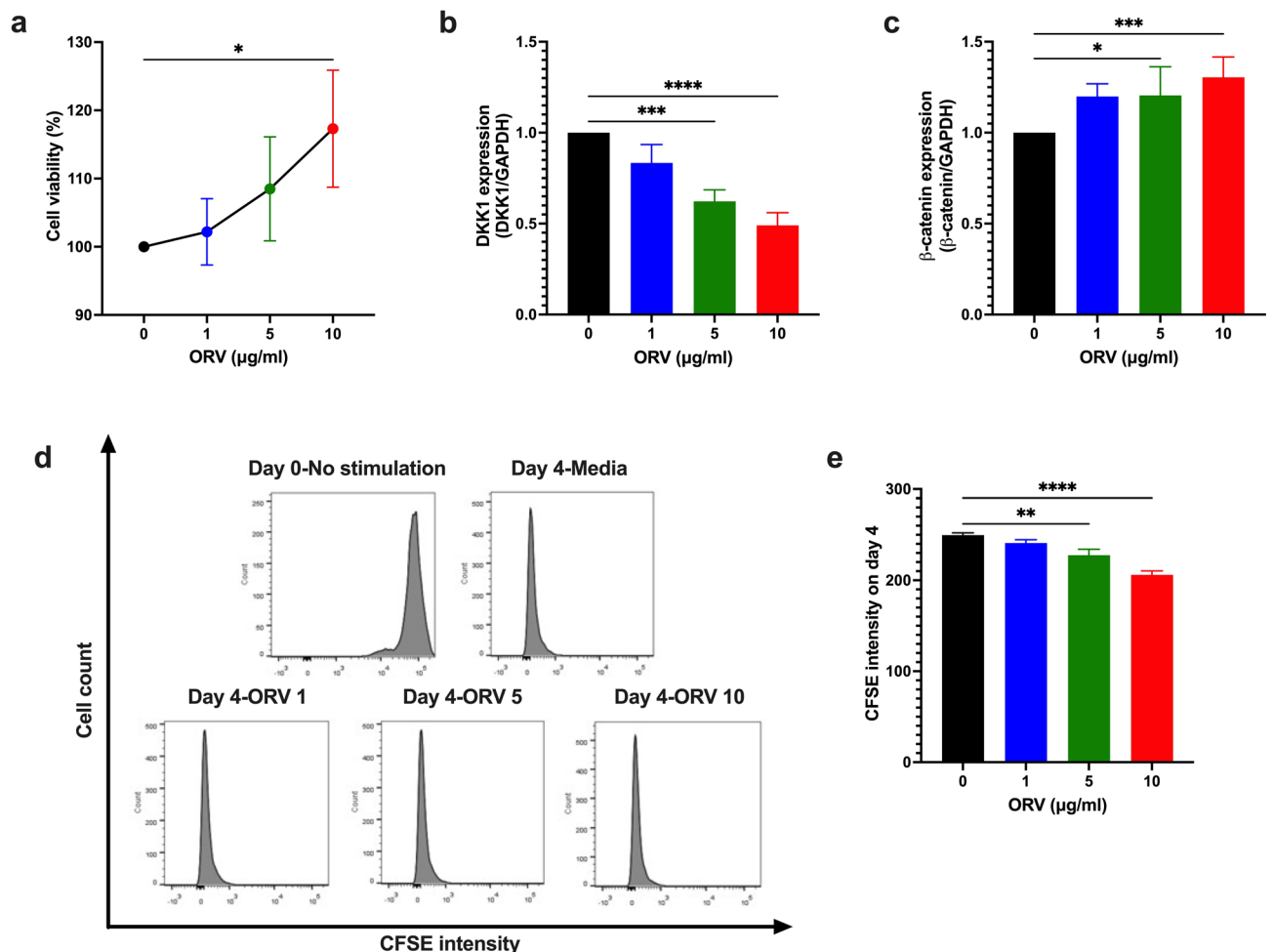


Fig. 1. The proliferative effect of ORV on HFDPCs. A significant of cell proliferation after treated with ORV for 24 h (a). Treating cells with ORV reduced the expression of DKK1 mRNA (b) and increased the expression of β -catenin mRNA (c). ORV stimulates the proliferation of HFDPCs marked by the significant reduction of CFSE fluorescent intensity after 4 days of treatment (d,e). * $P < 0.05$, ** $P < 0.01$, *** $P < 0.001$, **** $P < 0.0001$.

Oxyresveratrol treatment reduces hair loss in an androgenetic alopecia mouse model

To evaluate the effect of ORV in an *in vivo* model, we used C57BL/6Njcl mice. The study was divided into two stages. In the first stage we aimed to determine the optimal concentration of ORV using mice that were simply shaved. The lotion concentration that stimulated the fastest hair growth was selected for the second stage (Fig. 5a,b).

In the second stage, an AGA mouse model was created by administering weekly DHT injections. The treatment lotion was applied to the dorsal area of the mice every other day. Minoxidil 3% was used as a standard treatment for comparison. Hair growth rate was assessed by the rate of change in dark area coverage over time. The minoxidil + ORV lotion resulted in the fastest hair growth, achieving full coverage by day 70. Lotions containing either ORV or minoxidil alone showed slower hair growth, with no significant difference between these two groups (Fig. 5c,d). In the AGA control group, dermoscopic images revealed areas of hair loss and broken hairs leaving black dots, this phenomenon not observed in the treatment groups (Fig. 5e).

Histological analysis indicated significant differences between the treatment groups and the AGA control in terms of the number of hair bulbs per mm, hair bulb diameter, and skin thickness (Fig. 6a). The highest number of hair bulbs per mm was observed in the minoxidil + ORV lotion group (20 ± 3.27), while the groups treated with either ORV or minoxidil alone showed no significant difference from each other (16 ± 2.97 vs. 17 ± 3.42 , respectively) (Fig. 6b). However, there were no significant differences among the three treatment groups regarding hair bulb diameter and skin thickness (Fig. 6c,d).

Discussion

Dermal papilla cells (DPCs), a subset of mesenchymal cells in the skin, play a critical role in regulating hair follicle development and growth. They also serve as a reservoir of multipotent stem cells, making them highly relevant in hair regeneration research^{24,25}. Clinically, the size of the dermal papilla is reduced in balding follicles, as seen in conditions like AA and AGA²⁶. Located at the base of the hair follicle, DPCs function as a signaling

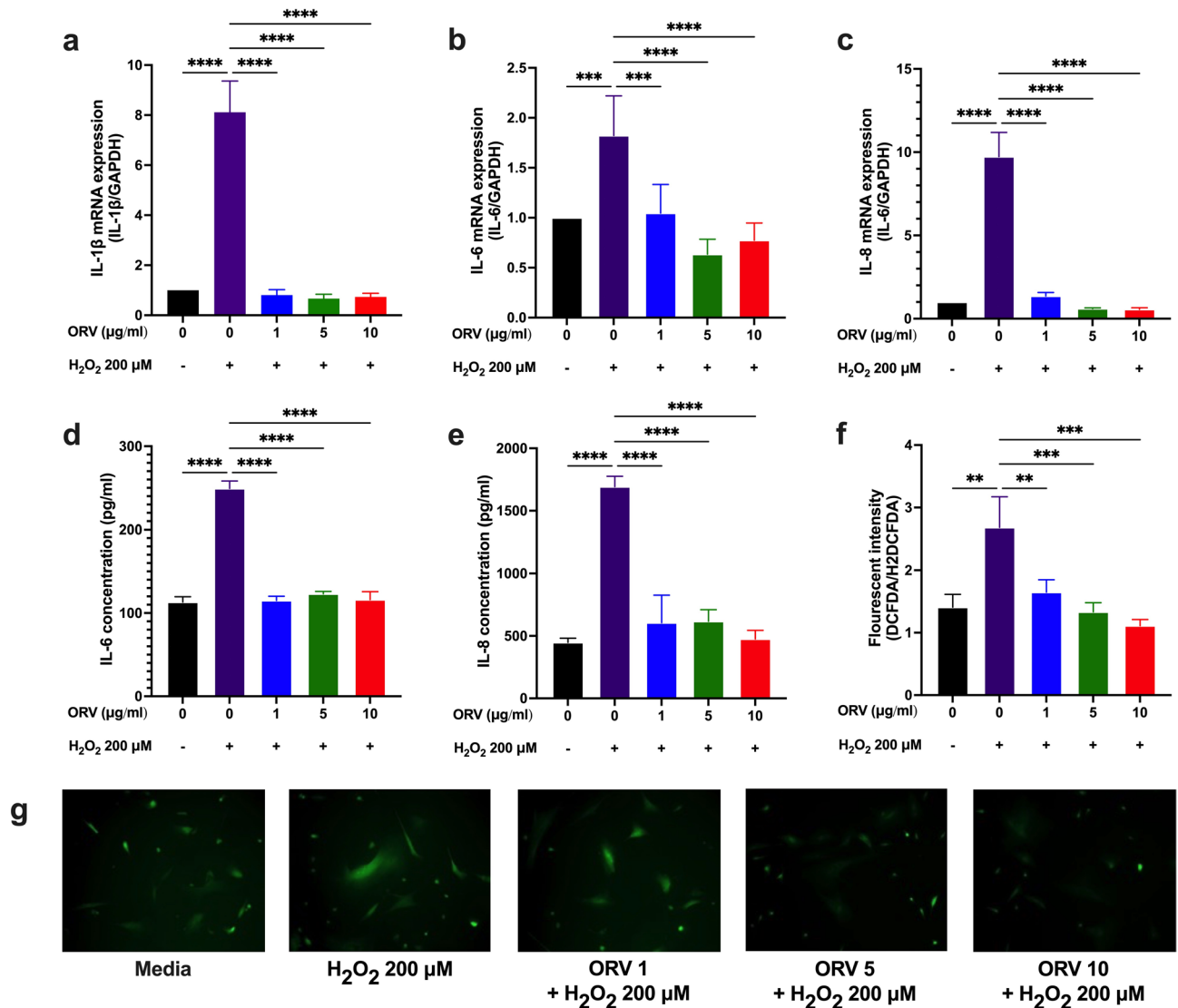


Fig. 2. The anti-inflammation effect of ORV due to oxidative stress. Oxidative stress was induced by treating cells with H₂O₂ 200 μM. Pretreating HFDPCs with ORV from 1 to 10 μg/ml for 24 h reduced the expression of mRNA IL-1β (a), IL-6 (b) and IL-8 (c). The production of IL-6 (d) and IL-8 (e) to supernatant were inhibited by ORV treatment. ORV helps to reduce ROS production due to H₂O₂ stimulation: quantification of mean fluorescent intensity of each group measured by a microplate reader (f), photographs taken by fluorescent microscope (g); ***P* < 0.01, ****P* < 0.001, *****P* < 0.0001.

hub, orchestrating hair growth by secreting factors that regulate the proliferation of adjacent hair matrix cells. Thus preserving the inductive potential of DPCs *in vitro* is essential for successful hair follicle morphogenesis and regeneration²⁷.

ORV, a potent antioxidant, has shown the dermatological benefits due to anti-inflammatory and antioxidant properties, making it a potential candidate for treating various medical conditions, including alopecia which often involve inflammation^{16,20,21,23}. In this study, we explored the effects of ORV on hair loss using HFDPCs and C57BL/6Njcl mouse model.

Our study demonstrates that ORV significantly increased proliferation of normal HFDPCs at concentration of 10 μg/ml, consistent with previous studies on other cell lines^{17,23}. The cell growth-promoting effect was validated through MTT assay and CFSE assay. β-catenin, a key player in hair follicle development, is crucial for promoting the anagen phase of hair cycle and regulating keratinocyte differentiation²⁸. DKK1, a known antagonist of the Wnt/β-catenin signaling pathway, inhibits hair follicle proliferation by downregulating β-catenin²⁹. In our study, ORV treatment led to a reduction DKK1 expressin and upregulation of β-catenin, promoting the proliferation of HFDPCs.

We also established an oxidative stress-induced AA model in HFDPCs using 200 μM H₂O₂³⁰. ORV significantly inhibited the production of various pro-inflammatory cytokines, including IL-1β, IL-6, and IL-8, at both mRNA and protein levels. Furthermore, the DCFDA assay confirmed that ORV reduced ROS levels, which

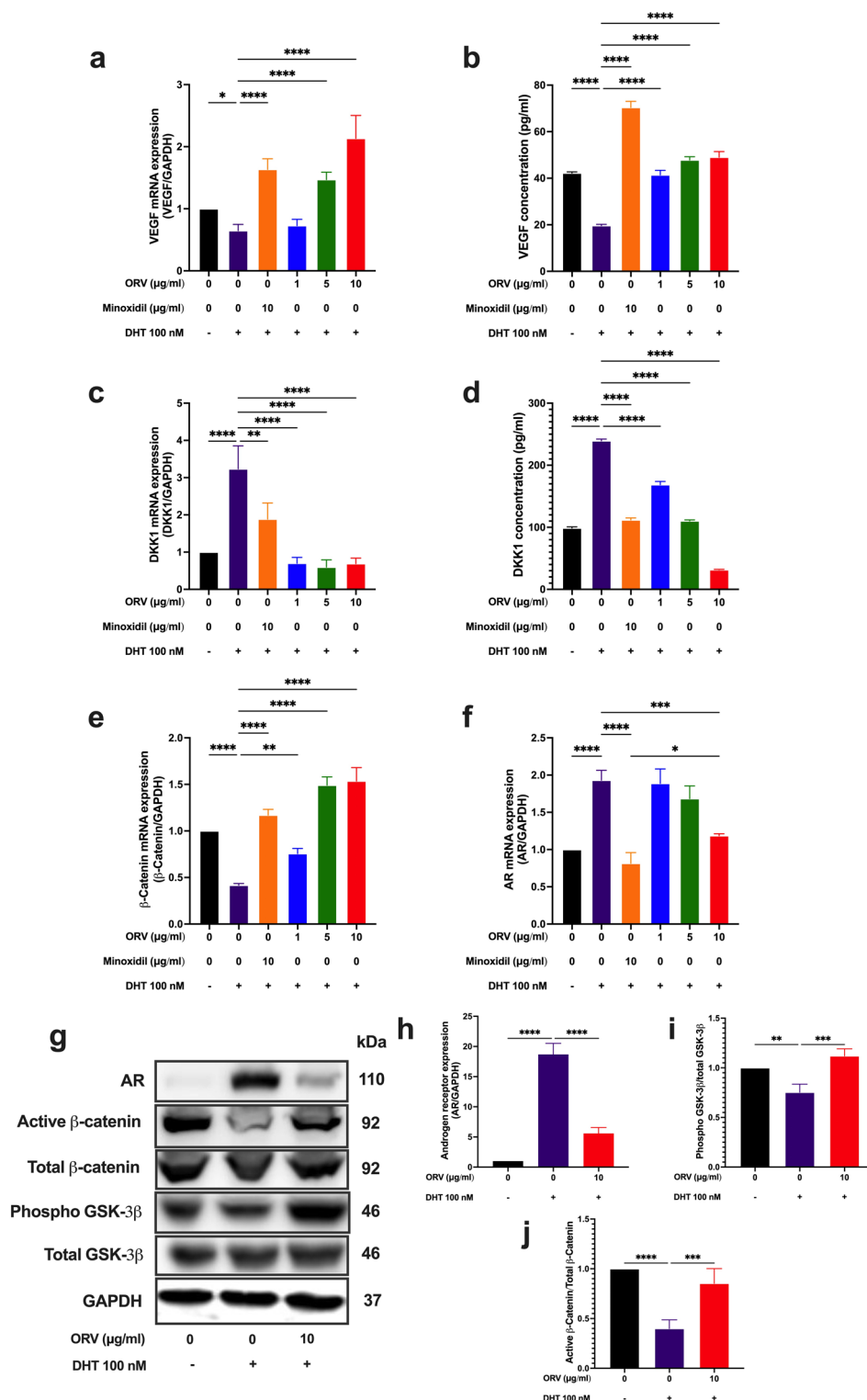


Fig. 3. Effect of ORV on DHT-induced HFDFCs senescence. HFDFCs were treated with ORV at concentration 1, 5 and 10 μg/ml for 30 min, followed by expose to 100 nM DHT for 24 h. The ORV-pretreated group showed an increase in stimulating factors for HFDFCs regeneration including VEGF (a,b) and mRNA of β-catenin (e). Conversely, pretreatment with ORV reduced the expression of HFDFC growth inhibiting factors including DKK1 (c,d) and mRNA of AR (f). Western-blot analysis was performed to determine the intracellular impact of ORV under DHT stimulation (g). The result revealed a decrease of AR protein expression level (h) and increase in the ratio of phosphorylated GSK-3β/total GSK-3β as well as the ratio of non-phosphorylated (active) β-catenin/β-catenin total in the ORV-pretreated group (i,j). GAPDH was used as the internal control. * $P < 0.05$, ** $P < 0.01$, *** $P < 0.001$, **** $P < 0.0001$.

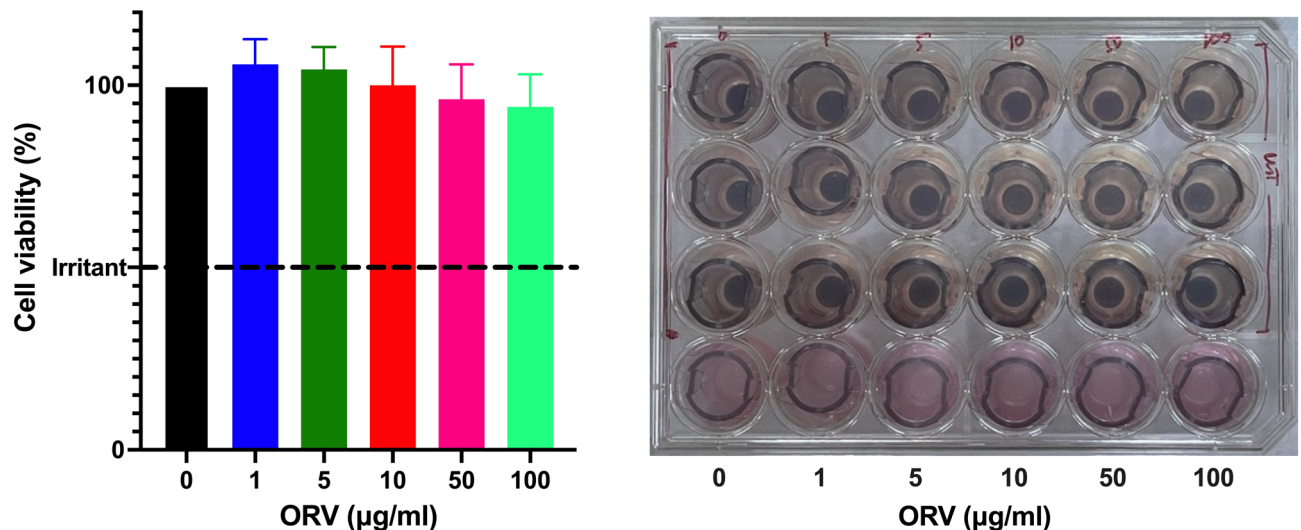


Fig. 4. Skin irritation test. A 3-D human cultured epidermis model was utilized to evaluate the irritant potential of ORV. The epidermal tissues were treated with ORV solutions at concentrations of 1, 5, 10, 50, and 100 µg/ml for 42 h. The mean relative tissue viability of three individual tissues exposed to the test substance was determined using an MTT assay. A tissue viability of $\leq 50\%$ is defined as indicative of irritation.

are known to trigger inflammation through NF- κ B activation, a central regulator of inflammatory response³¹. This suggests that ORV's anti-inflammatory effects, mediated through the NF- κ B inhibition and may play a critical role in its therapeutic potential, as supported by similar findings in keratinocytes and macrophages^{23,32}.

DHT, which binds to AR with highest affinity, is a primary factor in AGA pathogenesis. The binding of DHT to AR upregulates inhibitors of HFDPs proliferation such as DKK-1 and IL-6, leading to hair follicle regression³³. The upregulation of DKK-1 is particularly significant as it inhibits the Wnt/ β -catenin signaling pathway, thereby halting the proliferation of HFDPs³⁴. Our results revealed that ORV at 10 µg/ml effectively suppressed DKK-1 expression while enhancing VEGF mRNA expression and maintaining VEGF production in HFDPs at levels comparable to control. VEGF, a key mediator of angiogenesis, plays a pivotal role in stimulating hair regeneration³⁵. ORV's influence on both VEGF and DKK-1 was observed at both the mRNA and protein levels.

In addition, DHT stimulation increases AR production in HFDPs, further exacerbating AGA³⁶. Our study demonstrated that ORV could suppress AR production, contributing to preservation of HFDPs proliferation. Furthermore, the Wnt/ β -catenin signaling pathway, which is vital for hair follicle morphogenesis and growth, was modulated by ORV. The phosphorylation of GSK-3 β , which inhibits β -catenin degradation, was induced by ORV, thereby stabilizing β -catenin and promoting hair follicle proliferation^{37,38}. These findings highlight ORV's potential in modulating key pathways involved in hair growth, positioning it as a promising therapeutic candidate for AGA.

Before progressing to *in vivo* experiments with mice, we evaluated the irritant potential of ORV using a 3D human cultured epidermis model. According to the GHS standard, the MTT assay confirmed that ORV did not induce skin irritation, thereby establishing it as a safe candidate for further study³⁹.

Given AGA's significant impact on quality of life and lack of a definitive treatment, we applied our findings to an *in vivo* model. We developed a lotion containing ORV and compared its efficacy with minoxidil, the only FDA-approved topical treatment for AGA⁴⁰. Previous studies have shown that DHT treatment leads to thinner dorsal skin, reduced hair follicle proliferation, and increased apoptosis in C57BL/6 mice⁴¹. We utilized DHT-induced AGA mice to investigate whether ORV can help regenerate hair follicles. In our DHT-induced AGA mouse, both ORV and 3% minoxidil demonstrated equivalent effectiveness in promoting hair growth. Furthermore, the combined lotion of ORV and minoxidil produced superior results. Histological analysis revealed that ORV was as effective as minoxidil in maintaining dorsal skin thickness and increasing the size and number of hair bulbs. This finding is consistent with *in vitro* findings of ORV-induced DPC proliferation through the β -catenin signaling pathway.

This study is the first to demonstrate the regenerative effect of ORV on DPCs and hair follicles alopecia models, suggesting its potential as a promising treatment for hair loss primarily through the β -catenin signaling pathway (Fig. 7). Future clinical studies in individuals with alopecia are necessary to validate the safety, efficacy and practical applicability of ORV-based therapy for hair loss.

Materials and methods

Culture of hair follicle dermal papilla cell

All the media and reagents for HFDPs culture were purchased from Cell Applications (#602K-05a, San Diego, CA, USA). Cells were incubated at 37 °C in a humidified incubator containing 5% CO₂. Cells were pre-treated

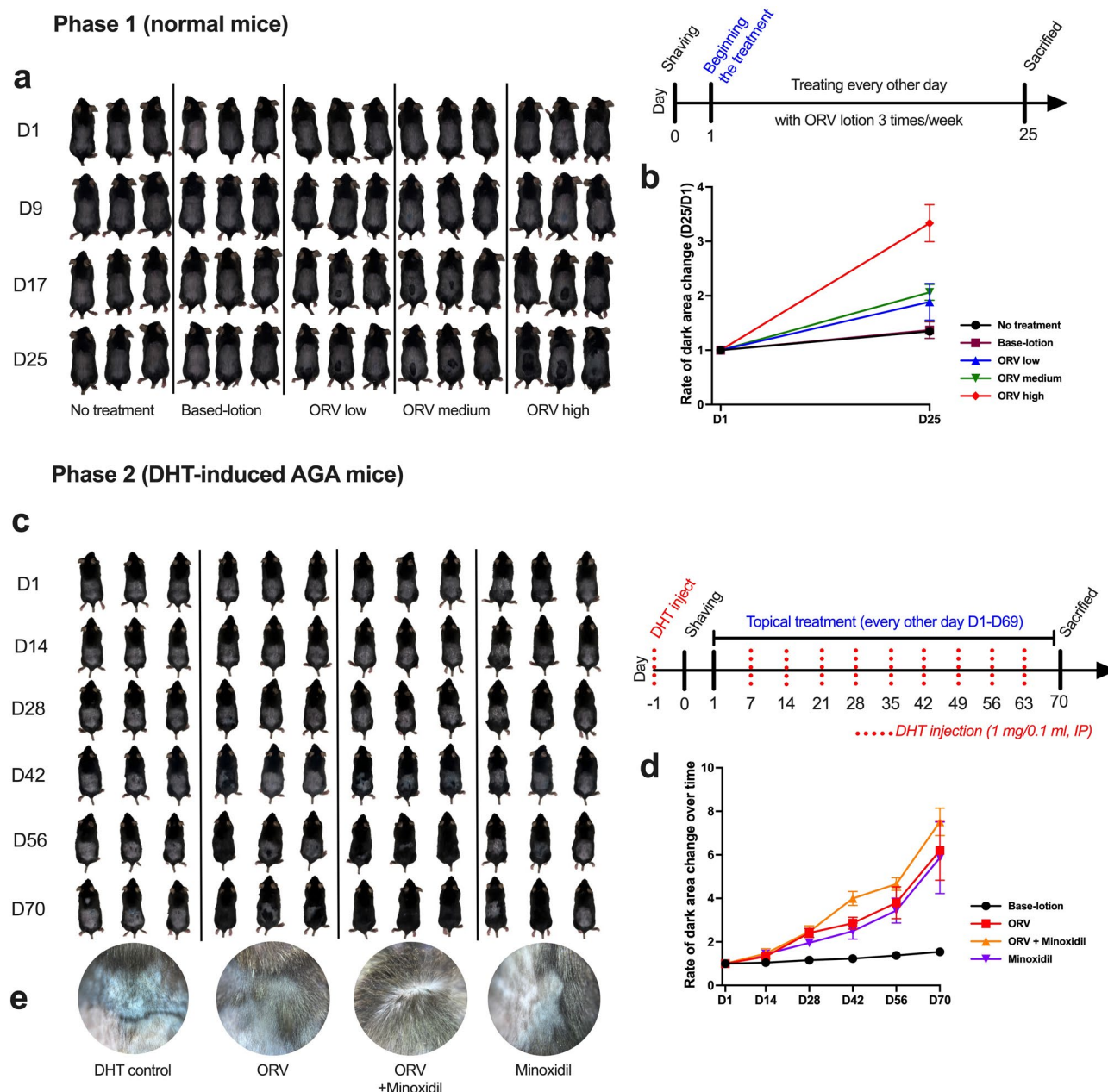


Fig. 5. Effect of ORV on hair regeneration in AGA mice. The mice were initially tested with several doses of ORV to choose the optimal concentration for subsequent experiments (a,b). Selected concentration of ORV was used for the next phase with AGA model (c,d). At the conclusion of the treatment, dermoscopic images were taken to assess the condition of hair follicles (e).

with ORV for 24 h before exposed to DHT for next 24 h. Then, samples were collected for further experiments. The cellular passage did not exceed six occurrences across all experiments.

Reagents

Oxyresveratrol

ORV from *Artocarpus lakoocha*, was kindly given by the Thailand's Ministry of Public Health. The purity of ORV was analyzed using ultra-performance liquid chromatography and had a purity greater than 95%. For the *in vitro* cell culture experiment, ORV was dissolved in dimethyl sulfoxide (DMSO) and diluted with phosphate buffer saline (PBS) to achieve the working concentration, with the final concentration of DMSO in the solution was less than 1%. For the *in vivo* experiment on mouse hair regeneration model, ORV lotions were developed by Faculty of Medicine, Chulalongkorn University.

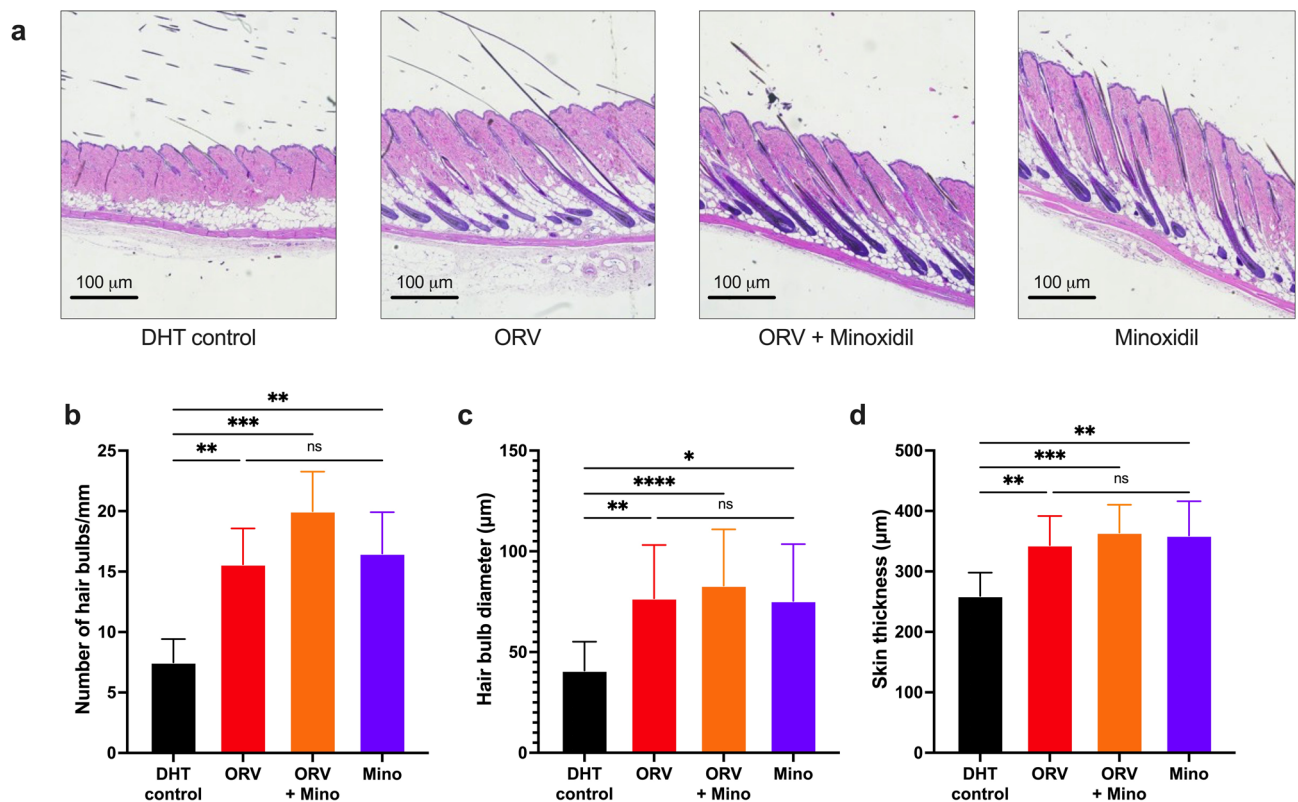


Fig. 6. ORV prevented the effects of DHT on the skin and hair follicles. Skin samples were collected and subjected to hematoxylin and eosin staining, with histological images presented at $\times 200$ magnification (a). Quantitative analysis included the number of hair bulbs, hair bulb diameter, and skin thickness across the different treatment groups (b–d). ** $P < 0.01$, *** $P < 0.001$, **** $P < 0.0001$.

Dihydrotestosterone

DHT commercially known as Stanolone (#A0462), was produced by TCI, Japan. The compound was dissolved in DMSO and diluted with PBS to reach the desired working concentration.

Minoxidil

Minoxidil (#M1389, TCI, Japan) was used as the standard control in this study. The compound was dissolved in ethanol and diluted with PBS for the *in vitro* cell culture experiment. For the mouse experiment, lotion containing minoxidil was also developed by Faculty of Medicine, Chulalongkorn University.

Cell viability assay

To detect the cytotoxicity of ORV to HFDPCs, we seed 0.5×10^4 cells/well in a flat-bottom 96-well plate (SPL Life Sciences, Gyeonggi-do, Korea) with HFDPCs Growth Medium (#611-500, Cell Applications, San Diego, CA, USA) at 37°C in a humid 5% CO_2 atmosphere for 24 h. Then, cells were treated with ORV at desired concentrations as determined in our previous study on keratinocytes²³. Fifty microliters of MTT reagent (3-(4,5-dimethylthiazol-2-yl)-2,5-diphenyltetrazolium bromide) (#ab211091, Abcam Plc., Aibo Trading Co., Ltd., Shanghai, China) was added to each well and incubate in a 5% CO_2 incubator at 37°C for 3 h. Next, optical densities (OD) were measured at a wavelength of 490 nm using Varioskan microplate reader (Thermofisher Scientific, Grand Island, NY, USA).

Cell proliferation assay

The proliferation assay was performed on HFDPCs using CFSE Cell Division Tracker kit (#423801, BioLegend, San Diego, CA, USA). Cells were stained with CFSE (5-(and 6)-Carboxyfluorescein diacetate succinimidyl ester) before being cultured in 6-well plate (SPL Life Sciences, Gyeonggi-do, Republic of Korea) and incubated overnight. The next day, the cells were treated with ORV for 48 h. Before analysis, the cells were trypsinized and washed with PBS. The cells were then resuspended in FACs buffer and the intensity of CFSE was measured using BD[®] LSR II flow cytometer (BD Biosciences, Franklin Lakes, NJ, USA). Data was analyzed using FlowJo 10 cytometry analysis software (FlowJo, Ashland, OR, USA).

RNA isolation, complementary DNA synthesis, quantitative real time-PCR analysis

Total RNA from cells was isolated using TRIzol reagent (Gibco, Carlsbad, CA, USA) according to the manufacturer's instructions. The first strand of cDNA was synthesized from 500 ng total RNA using iScript[™]

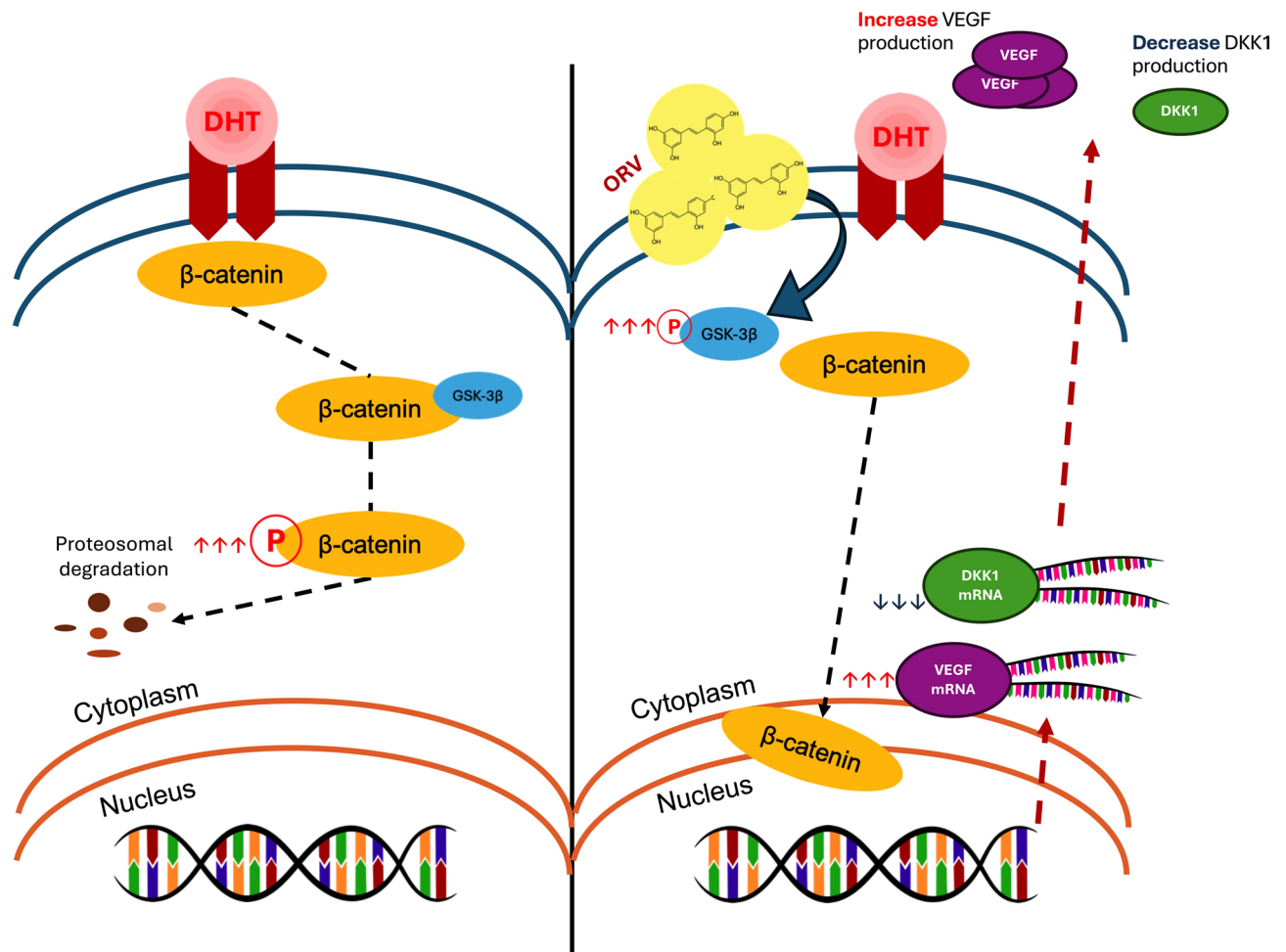


Fig. 7. Diagram of mechanism of ORV in counteracting DHT-induced AGA in HFDPCs. ORV effectively counters the degradation of β -catenin induced by DHT by promoting the phosphorylation of GSK-3 β , thereby preventing its interaction with β -catenin. This stabilization allows the active, non-phosphorylated β -catenin to translocate into the nucleus, where it facilitates the proliferation of HFDPCs. Additionally, ORV enhances the production of VEGF, a key factor in promoting hair regeneration, while simultaneously suppressing DKK1, a critical inhibitor of hair growth.

cDNA Synthesis kit (#1708891, Biorad, Hercules, CA, USA). For real time-PCR, the amplification steps were performed using iScript™ Reverse Transcription Supermix (#1708841, Biorad, Hercules, CA, USA) as follows: 1 cycle at 95 °C for 10 min, 40 cycles at 95 °C for 30 s, 60 °C for 30 s, and 72 °C for 1 min (Table 1).

Enzyme-linked immunosorbent assay (ELISA)

The levels of supernatant cytokines and protein were measured using human IL-6 and IL-8 ELISA kits (#88-7066 and #8086-22, respectively; Thermofisher Scientific, Carlsbad, CA, USA), DKK1 ELISA kit (#DKK100B, R&D systems, Minneapolis, MN, USA), VEGF ELISA kit (#466507, BioLegend, San Diego, CA, USA). Cell cultures were performed in triplicate for each treatment condition. Concentrations were calculated using the standard curve generated by a curve-fitting program.

ROS generation detection

ROS formation in HFDPCs was detected using a DCFDA/H2DCFDA-Cellular ROS Assay Kit (ab113851, Abcam, Cambridge, UK) according to the manufacturer's protocol. Fluorescent intensity was measured by Varioskan microplate reader (Thermofisher Scientific, Grand Island, NY, USA) at Ex/Em = 485/535 nm.

Western blot analysis

Western blot was utilized to collect intracellular protein. Cells were lysed with RIPA buffer (#9806, Cell Signaling Technology, Danvers, MA, USA) containing protease/phosphatase inhibitor cocktail (#5872, Cell Signaling Technology, Danvers, MA, USA). Protein concentration was determined using BCA Protein Assay kit (#7780, Cell Signaling Technology, Danvers, MA, USA). Twenty μ g of protein lysate was loaded onto 8–12% SDS-PAGE. The protein was then transferred to nitrocellulose membrane (#1620112, Biorad, Hercules, CA, USA) at 70 volts for 75 min. The membrane was then blocked with 5% nonfat dry milk (#9999, Cell Signaling Technology,

Gene	Sequence	T _m (°C)	Length (base pairs)
<i>GAPDH</i>	Fw: 5'-ACC CAC TCC TCC ACC TTT-3' Rv: 5'-CAC CAC CCT GTT GCT GTA G-3'	60	108
<i>IL-1β</i>	Fw: 5'-ACA GAT GAA GTG CTC CTT CCA-3' Rv: 5'-GTC GGA GAT TCG TAG CTG GAT-3'	60	73
<i>IL-6</i>	Fw: 5'-GGC ACT GGC AGA AAA CAA CC-3' Rv: 5'-GCA AGT CTC CTC ATT GAA TCC-3'	60	85
<i>IL-8</i>	Fw: 5'-GAG AGT GAT TGA GAG TGG ACC AC-3' Rv: 5'-CAC AAC CCT CTG CAC CCA GTT T-3'	60	112
<i>AR</i>	Fw: 5'-CTC TCA CAT GTG GAA GCT GCA AG-3' Rv: 5'-TTT CCG AAG ACG ACA AGA TGG AC-3'	60	137
<i>VEGF</i>	Fw: 5'-GCC AGC ACA TAG GAG AGA TG-3' Rv: 5'-CAC GCT CCA GGA CTT ATA CC-3'	60	155
<i>β-catenin</i>	Fw: 5'-TTA GCT GGT GGG CTG CAG AA -3' Rv: 5'-GGG TCC ACC ACT AGC CAG TAT GA-3'	60	141
<i>DKK-1</i>	Fw: 5'-ATG CGT CAC GCT ATG TGC TG-3' Rv: 5'-TGG AAT ACC CAT CCA AGG TGC TA-3'	60	145

Table 1. Sequence of primers used in this study.

Danvers, MA, USA) in 1× TBST for 60 min at room temperature and then incubated with primary antibodies at 4 °C overnight. Primary antibodies were used in the study included: GAPDH (D16H11) XP[®] rabbit mAb (#5174), Androgen Receptor (D6F11) XP[®] Rabbit mAb (#5153), β-Catenin (D10A8) XP[®] Rabbit mAb (#8480), Non-phospho (Active) β-Catenin (Ser33/37/Thr41) (D13A1) Rabbit mAb (#8814), GSK-3β (D5C5Z) XP[®] Rabbit mAb (#12456), Phospho-GSK-3β (Ser9) (D85E12) XP[®] Rabbit mAb (#5558). The following day, the membrane was incubated in blocking buffer containing HRP-conjugate anti-rabbit secondary antibody (#7074) followed by washing steps. All antibodies were purchased from Cell Signaling Technology (Danvers, MA, USA). Protein bands were detected using UltraScience Pico Plus Western Substrate (Bio-Helix, New Taipei City, Taiwan). GAPDH expression levels were used as an internal control. Band intensity of the proteins of interest was quantified from triplicate Western blot images using Image Lab software version 6.1 (Bio-Rad Laboratories, Hercules, CA, USA).

Skin irritation test with 3-D human cultured epidermis

A 3-D human cultured epidermis model (Labcyte EPI-MODEL 6D, Japan Tissue Engineering Co., Ltd (J-TEC)) was employed to assess the irritant potential of ORV before applying the substance to mouse skin at a broader range of concentrations than previously studied. Initially, the human epidermal tissues were incubated in a CO₂ incubator for 24 h. Subsequently, various concentrations of the ORV solution were applied to the surface of the epidermal tissues, ensuring even distribution across the entire tissue, and incubated for an additional 42 h. Post-incubation, the tissues were rinsed three times with PBS, followed by an MTT assay as per the manufacturer's protocol. According to the Globally Harmonized System of Classification and Labeling of Chemicals (GHS), a substance is considered an irritant if the mean relative tissue viability of three individual tissues exposed to the test substance is reduced to below 50% of the mean viability of the negative controls.

Mouse model

Seven-to-nine-week-old C57BL/6Njcl mice were purchased from Nomura Siam (Bangkok, Thailand). The animals were maintained according to the standard animal care protocol approved by the Animal Care and Use Committee of the Faculty of Medicine, Chulalongkorn University (No. 039/3566; approved on December 2023). Mice were housed in a husbandry unit with a 12 h light/dark cycle under thermoregulated (22 ± 2 °C) and humidity-controlled (50 ± 10%) condition and provided with standard diet and water ad libitum. Throughout the procedure, the mice were maintained under anesthesia using isoflurane administered via a ventilator. At the conclusion of each phase, the mice were humanely euthanized using the cervical dislocation method.

Finding out the optimal concentration of ORV (Phase 1)

All mice were randomly assigned to five groups: no treatment, based-lotion, ORV low, ORV medium, ORV high, with 3 mice in each group. After grouping, the mice had their back fur shaved. Then, lotion was applied every other day for 3 weeks. The lotion formulation that promoted the fastest hair growth was selected for the next phase of the study. Hair growth rate was assessed using Image J.

Effect of ORV on hair regeneration with androgenetic alopecia model (Phase 2)

The ORV lotion with the optimal concentration identified in Phase 1 will be used in Phase 2. Mice were randomly assigned to four groups: no treatment control, ORV lotion, ORV + minoxidil lotion, and minoxidil lotion. To create the AGA model, all mice had their back fur shaved and were injected with DHT at a dose of 1 mg per week. Subsequently, the treatment lotion was applied every other day to monitor its efficacy in stimulating hair growth. Hair growth rate was assessed by Image J.

Pathology observation

The dorsal skin was fixed in 4% paraformaldehyde for 24 h prior to being embedded in paraffin. The paraffin-embedded skin sections were mounted on glass slides and stained with hematoxylin and eosin (H&E) to analyze the histology, skin thickness, hair bulb characteristics.

Statistical analysis

Statistical analysis was performed using GraphPad Prism version 9.0. For multiple comparison test, one-way ANOVA was used. Pairwise comparisons were also performed to determine the statistical significance of different ORV concentration groups. Unless otherwise noted, data were collected from triplicate samples, and numerical values were presented in graphical formats as mean \pm standard deviation (SD). Difference was considered statistically significant when the *p* value was less than 0.05.

Data availability

The data are available from the first and corresponding authors upon reasonable request.

Received: 5 November 2024; Accepted: 14 May 2025

Published online: 20 May 2025

References

- Gupta, A. K., Ravi, P., Wang, T. & S. & Alopecia areata and pattern hair loss (androgenetic alopecia) on social media – Current public interest trends and cross-sectional analysis of YouTube and TikTok contents. *J. Cosmet. Dermatol.* **22**, 586–592. <https://doi.org/10.1111/jocd.15605> (2023).
- Browning, J. D. *Dermatology* Edited by Jean L. Bologna Julie V. Schaffer Lorenzo Cerroni Fourth edition China: Elsevier, 2018, ISBN 978-0-7020-6275-9. *Pediatr. Dermatol.* **35**, 289–289. <https://doi.org/10.1111/pde.13439> (2018).
- Villasante Fricke, A. C. & Miteva, M. Epidemiology and burden of alopecia areata: a systematic review. *Clin. Cosmet. Investig. Dermatol.* **8**, 397–403. <https://doi.org/10.2147/ccid.S53985> (2015).
- Lundin, M. et al. Gender differences in alopecia areata. *J. Drugs Dermatol.* **13**, 409–413 (2014).
- Kabir, Y. & Goh, C. Androgenetic alopecia: update on epidemiology, pathophysiology, and treatment. *J. Egypt. Women's Dermatol. Soc.* **10**, 107–116. <https://doi.org/10.1097/01.EWX.0000432183.50644.f6> (2013).
- Salman, K. E., Altunay, I. K., Kucukunal, N. A. & Cerman, A. A. Frequency, severity and related factors of androgenetic alopecia in dermatology outpatient clinic: hospital-based cross-sectional study in Turkey. *Bras. Dermatol.* **92**, 35–40. <https://doi.org/10.1590/abd1806-4841.20175241> (2017).
- Biran, R., Zlotogorski, A. & Ramot, Y. The genetics of alopecia areata: new approaches, new findings, new treatments. *J. Dermatol. Sci.* **78**, 11–20. <https://doi.org/10.1016/j.jdermsci.2015.01.004> (2015).
- Bertolini, M., McElwee, K., Gilhar, A., Bulfone-Paus, S. & Paus, R. Hair follicle immune privilege and its collapse in alopecia areata. *Exp. Dermatol.* **29**, 703–725. <https://doi.org/10.1111/exd.14155> (2020).
- Zhang, X. et al. Development of alopecia areata is associated with higher central and peripheral hypothalamic-pituitary-adrenal tone in the skin graft induced C3H/HeJ mouse model. *J. Invest. Dermatol.* **129**, 1527–1538. <https://doi.org/10.1038/jid.2008.371> (2009).
- Peterle, L., Sanfilippo, S., Borgia, F., Cicero, N. & Gangemi, S. Alopecia areata: A review of the role of oxidative stress, possible biomarkers, and potential novel therapeutic approaches. *Antioxidants* **12**, 135 (2023).
- Ntshingila, S., Oputu, O., Arowolo, A. T. & Khumalo, N. P. Androgenetic alopecia: an update. *JAAD Int.* **13**, 150–158. <https://doi.org/10.1016/j.jdin.2023.07.005> (2023).
- Jung, Y. H. et al. Cyanidin 3-O-arabinoside suppresses DHT-induced dermal papilla cell senescence by modulating p38-dependent ER-mitochondria contacts. *J. Biomed. Sci.* **29**, 17. <https://doi.org/10.1186/s12929-022-00800-7> (2022).
- Kwon, Y. E., Choi, S. E. & Park, K. H. Regulation of cytokines and dihydrotestosterone production in human hair follicle papilla cells by supercritical extraction-Residues extract of *Ulmus davidiana*. *Molecules* **27** <https://doi.org/10.3390/molecules27041419> (2022).
- Ding, Y. W., Li, Y., Zhang, Z. W., Dao, J. W. & Wei, D. X. Hydrogel forming microneedles loaded with VEGF and Ritlecitinib/polyhydroxyalkanoates nanoparticles for mini-invasive androgenetic alopecia treatment. *Bioactive Mater.* **38**, 95–108. <https://doi.org/10.1016/j.bioactmat.2024.04.020> (2024).
- Shin, D. W. The molecular mechanism of natural products activating Wnt/ β -Catenin signaling pathway for improving hair loss. *Life (Basel)*. **12** <https://doi.org/10.3390/life12111856> (2022).
- Chatsumpun, N. et al. Oxyresveratrol: structural modification and evaluation of biological activities. *Molecules* **21**, 489–489. <https://doi.org/10.3390/molecules21040489> (2016).
- Likhitwitayawuid, K. Oxyresveratrol: Sources, productions, biological activities, pharmacokinetics, and delivery systems. *Molecules* **26**, 4212 (2021).
- Chung, K. O. et al. In-vitro and in-vivo anti-inflammatory effect of Oxyresveratrol from *Morus alba* L. *J. Pharm. Pharmacol.* **55**, 1695–1700. <https://doi.org/10.1211/0022357022313> (2003).
- Chen, C. C. et al. (2015).
- Hankittichai, P. et al. Oxyresveratrol inhibits IL-1 β -Induced inflammation via suppressing AKT and ERK1/2 activation in human microglia, HMC3. *Int. J. Mol. Sci.* **21**, 6054. <https://doi.org/10.3390/ijms21176054> (2020).
- Du, H., Ma, L., Chen, G. & Li, S. The effects of Oxyresveratrol abrogates inflammation and oxidative stress in rat model of spinal cord injury. *Mol. Med. Rep.* **17**, 4067–4073. <https://doi.org/10.3892/mmr.2017.8294> (2018).
- Wikan, N., Hankittichai, P., Thaklaewphan, P., Potikanond, S. & Nimlamool, W. Oxyresveratrol inhibits TNF- α -stimulated cell proliferation in human immortalized keratinocytes (HaCaT) by suppressing AKT activation. *Pharmaceutics*. **14**, 63 (2022).
- Tran, H. G. et al. Oxyresveratrol attenuates inflammation in human keratinocyte via regulating NF- κ B signaling and ameliorates eczematous lesion in DNCB-Induced dermatitis mice. *Pharmaceutics* **15**, 1709 (2023).
- Taghiabadi, E., Nilforoushzadeh, M. A. & Aghdami, N. Maintaining hair inductivity in human dermal papilla cells: A review of effective methods. *Skin Pharmacol. Physiol.* **33**, 280–292. <https://doi.org/10.1159/000510152> (2020).
- Driskell, R. R., Clavel, C., Rendl, M. & Watt, F. M. Hair follicle dermal papilla cells at a glance. *J. Cell Sci.* **124**, 1179–1182. <https://doi.org/10.1242/jcs.082446> (2011).
- Randall, V. A., The use of dermal & papilla cells in studies of normal and abnormal hair follicle biology. *Dermatol. Clin.* **14**, 585–594. [https://doi.org/10.1016/S0733-8635\(05\)70386-7](https://doi.org/10.1016/S0733-8635(05)70386-7) (1996).
- Schneider, M. R., Schmidt-Ullrich, R. & Paus, R. The hair follicle as a dynamic miniorgan. *Curr. Biol.* **19**, R132–R142. <https://doi.org/10.1016/j.cub.2008.12.005> (2009).

28. Bejaoui, M., Villareal, M. O. & Isoda, H. β -catenin-mediated hair growth induction effect of 3,4,5-tri-O-caffeoylquinic acid. *Aging (Albany NY)*. **11**, 4216–4237. <https://doi.org/10.18632/aging.102048> (2019).
29. Chu, H. Y. et al. Dickkopf-1: A promising target for Cancer immunotherapy. *Front. Immunol.* **12** <https://doi.org/10.3389/fimmu.2021.658097> (2021).
30. Zhang, Y. et al. Hair growth-promoting effect of resveratrol in mice, human hair follicles and dermal papilla cells. *Clin. Cosmet. Investig. Dermatol.* **14**, 1805–1814. <https://doi.org/10.2147/ccid.S335963> (2021).
31. Forrester, S. J., Kikuchi, D. S., Hernandez, M. S., Xu, Q. & Griending, K. K. Reactive oxygen species in metabolic and inflammatory signaling. *Circul. Res.* **122**, 877–902. <https://doi.org/10.1161/CIRCRESAHA.117.311401> (2018).
32. Lee, H. S., Kim, D. H., Hong, J. E., Lee, J. Y. & Kim, E. J. Oxyresveratrol suppresses lipopolysaccharide-induced inflammatory responses in murine macrophages. *Hum. Exp. Toxicol.* **34**, 808–818. <https://doi.org/10.1177/0960327114559989> (2015).
33. Chen, X. et al. Dihydrotestosterone regulates hair growth through the Wnt/ β -Catenin pathway in C57BL/6 mice and in vitro organ culture. *Front. Pharmacol.* **10** <https://doi.org/10.3389/fphar.2019.01528> (2020).
34. Giralt, I. et al. Dickkopf-1 inhibition reactivates Wnt/ β -catenin signaling in rhabdomyosarcoma, induces myogenic markers in vitro and impairs tumor cell survival in vivo. *Int. J. Mol. Sci.* **22**, 12921 (2021).
35. Gnann, L. A. et al. Hematological and hepatic effects of vascular epidermal growth factor (VEGF) used to stimulate hair growth in an animal model. *BMC Dermatol.* **13**, 15. <https://doi.org/10.1186/1471-5945-13-15> (2013).
36. Lee, D. K. & Chang, C. Expression and degradation of androgen receptor: mechanism and clinical implication. *J. Clin. Endocrinol. Metab.* **88**, 4043–4054. <https://doi.org/10.1210/jc.2003-030261> (2003).
37. Metcalfe, C. & Bienz, M. Inhibition of GSK3 by Wnt signalling—two contrasting models. *J. Cell Sci.* **124**, 3537–3544. <https://doi.org/10.1242/jcs.091991> (2011).
38. Liu, C. et al. Control of β -Catenin phosphorylation/degradation by a Dual-Kinase mechanism. *Cell* **108**, 837–847. [https://doi.org/10.1016/S0092-8674\(02\)00685-2](https://doi.org/10.1016/S0092-8674(02)00685-2) (2002).
39. Winder, C., Azzi, R. & Wagner, D. The development of the globally harmonized system (GHS) of classification and labelling of hazardous chemicals. *J. Hazard. Mater.* **125**, 29–44. <https://doi.org/10.1016/j.jhazmat.2005.05.035> (2005).
40. Devjani, S., Ezemma, O., Kelley, K. J., Stratton, E. & Senna, M. Androgenetic alopecia: therapy update drugs. **83**, 701–715. <https://doi.org/10.1007/s40265-023-01880-x> (2023).
41. Fu, D. et al. Dihydrotestosterone-induced hair regrowth Inhibition by activating androgen receptor in C57BL6 mice simulates androgenetic alopecia. *Biomed. Pharmacother.* **137**, 111247. <https://doi.org/10.1016/j.biopha.2021.111247> (2021).

Acknowledgements

This research is supported by the Second Century Fund (C2F), Chulalongkorn University, Bangkok, Thailand and funded by Thailand Science, Research, and Innovation Fund Chulalongkorn University (BCG_FF_68_068_3000_011) and Ratchadapiseksompotch Fund, Faculty of Medicine, Chulalongkorn University (GA65/74).

Author contributions

H.G.T.: Conceptualization, methodology, validation, formal analysis, investigation, writing-original draft. A.S. and K.R.: ORV resources. A.R.: Animal model study, K.M. and V.D.: writing-review. J.W.: Conceptualization, methodology, formal analysis, writing-review and editing, supervision, data curation, resources, project administration, funding acquisition.

Declarations

Ethics approval and consent to participate

The animal experiments in this study were approved by the Institutional Review Board in Animal Experiment of The Faculty of Medicine, Chulalongkorn University (No. 039/2566; approved on December 2022). All experiments were performed in accordance with the institution guideline and the principles outlined in the ARRIVE 2.0 guidelines to ensure transparency, reproducibility, and ethical standards in animal research.

Competing interests

The authors declare no competing interests.

Additional information

Supplementary Information The online version contains supplementary material available at <https://doi.org/10.1038/s41598-025-02581-z>.

Correspondence and requests for materials should be addressed to J.W.

Reprints and permissions information is available at www.nature.com/reprints.

Publisher's note Springer Nature remains neutral with regard to jurisdictional claims in published maps and institutional affiliations.

Open Access This article is licensed under a Creative Commons Attribution-NonCommercial-NoDerivatives 4.0 International License, which permits any non-commercial use, sharing, distribution and reproduction in any medium or format, as long as you give appropriate credit to the original author(s) and the source, provide a link to the Creative Commons licence, and indicate if you modified the licensed material. You do not have permission under this licence to share adapted material derived from this article or parts of it. The images or other third party material in this article are included in the article's Creative Commons licence, unless indicated otherwise in a credit line to the material. If material is not included in the article's Creative Commons licence and your intended use is not permitted by statutory regulation or exceeds the permitted use, you will need to obtain permission directly from the copyright holder. To view a copy of this licence, visit <http://creativecommons.org/licenses/by-nc-nd/4.0/>.

© The Author(s) 2025